JOURNAL OF MATERIALS SCIENCE 23 (1988) 3342–3347

Study by thermogravimetry, electrical conductivity and IR spectrometry of the phase transition for manganese cation deficient spinels

B. GILLOT, M. EL GUENDOUZI
Laboratoire de Recherches sur la Réactivité des Solides, Faculté des Sciences Mirande, B.P. 138, 21004 Dijon Cedex, France
M. LAARJ
Faculté des Sciences II, Université Hassan II, Casablanca, Morocco
P. TAILHADES, A. ROUSSET
Laboratoire de Chimie des Matériaux Inorganiques, Université Paul Sabatier, Toulouse III, 118 route de Narbonne, 31062 Toulouse Cedex, France

Thermogravimetry, electrical conductivity and IR spectrometry were used to study the crystal structure change of the metastable manganese cation deficient spinels that occur during the oxidation of manganese ions above 500° C. The kinetic of the transformation is found to be governed by a nucleation growth mechanism with an activation energy varying with the amount of Mn^{3+} ions. The nature of the inversion products depends on the manganese substitution extent. We observe for a substitution extent $x < 0.72$ a phase with a corundum structure which is a solid solution of α-$(MnFe)_2O_3$ and for $x > 0.72$ a mixture of two phases α-$(MnFe)_2O_3$ + Mn_2O_3 of orthorhombic structure.

1. Introduction

Several mixed oxides with a spinel structure containing iron (II) and substituted by divalent cations of the type $(M_x^{2+}Fe_{1-x}^{2+}Fe_2^{3+})O_4^{2-}$ with $0 < x < 1$ and $M^{2+} = Co^{2+}, Zn^{2+}, Mn^{2+}$, prepared at relatively low temperature (300° C) are very finely divided and, therefore, highly reactive with oxygen. If the oxidation of Fe^{2+} and Mn^{2+} ions is achieved below 400° C, which requires crystallite sizes of less than 200 nm, the oxidation reaction is topotactic with preservation of the spinel structure and in such instances it leads to the formation of defective phases γ [1]. Moreover, the oxidation process might be closely associated with the position of the Fe^{2+} and Mn^{2+} cations on the lattice [2] as it has been suggested that ions in tetrahedral sites (e.g. Fe^{2+}, Mn^{2+}) are strongly bound by covalent bonds, in contrast with the ionic bonding of octahedrally sited ions (as Fe^{2+}).

The purpose of this study was to investigate the crystal structure change of the manganese cation deficient spinels by increasing the oxidation temperature, eventually leading to a rhombohedral lattice (α-phase) which is stable at high temperature. The transformation mechanism will be more complicated than in the $\gamma \rightarrow \alpha - Fe_2O_3 + MFe_2O_4$ with M = Co, Zn because of the presence of manganese-ions, which leads to oxidation–reduction phenomena [2]. It has also been reported that for manganese aluminates first, a compound $\gamma(MnAl)_2O_3$ forms with distorted spinel structure [3], which gradually becomes γ-Al_2O_3 by diffusion of manganese ions out of the previous phase, and α-Al_2O_3 in the final phase.

2. Samples and experimental methods

The conditions of the preparation of finely grained manganese substituted magnetites have already been quoted in [2]. The synthesized materials have the cation distribution $(Mn_{0.8x}^{2+}Fe_{1-0.8x}^{3+})_A(Fe_{1+0.6x}^{3+}Fe_{1-0.8x}^{2+}Mn_{0.2x}^{3+})_BO_4^{2-}$ with Mn^{2+} ions on all the tetrahedral sites (A sites) and a small amount of Mn^{3+} ions on octahedral sites (B sites). Defect phases γ of the same spinel structure were obtained by low temperature oxidation (< 500° C) at $P_{O_2} = 10^4$ Pa of previously initial spinels. Thermogravimetric analysis indicated [2] that below 400° C, the weight change is due to total oxidation of Fe^{2+} in Fe^{3+} ions (about 200° C) and Mn^{3+} in Mn^{4+} ions (about 270° C) on B sites and an incomplete oxidation of Mn^{2+} in Mn^{3+} ions (about 350° C) on A sites (Fig. 1, region I). Between 400 and 500° C a loss in weight occurred according to the reduction of Mn^{4+} to Mn^{3+} ions (Fig. 1, region II). For the two regions, X-ray analysis should show a single phase of spinel structure. The formula of defective manganese substituted magnetites can be structurally represented as follows

$$[Mn_{8x/(9-0.32x)}Fe_{(24-8x)/(9-0.32x)}\square_{(3-0.96x)/(9-0.32x)}]0_4^{2-}$$

where □ is the vacant site.

0022–2461/88 $03.00 + .12

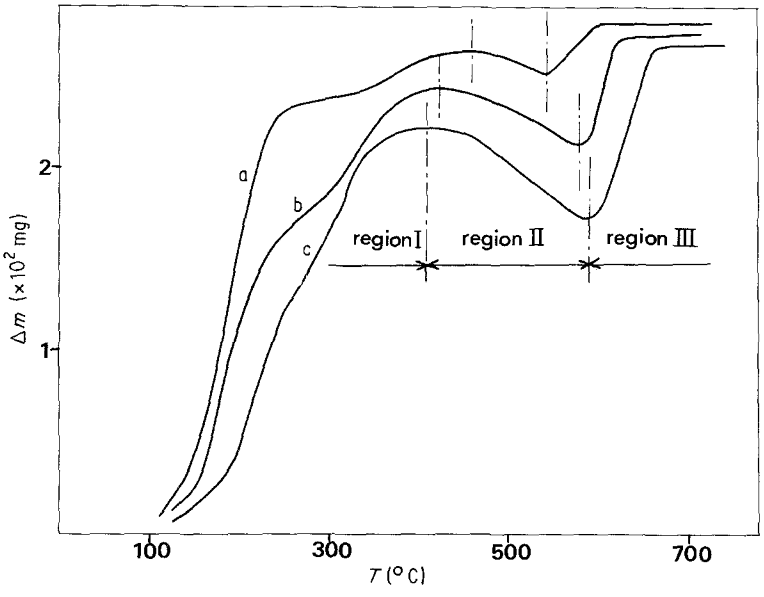

Figure 1 *TG* curves for manganese-substituted magnetites heated in air at 2.5°C min^{-1} (a $x = 0.27$, b $x = 0.50$, c $x = 0.97$).

Above 500° C, we again have a weight gain (Fig. 1, region III) attributed to the oxidation of Mn^{2+} ions that were not completely oxidized at lower temperature and this reaction is accompanied by a phase change. The oxidation mechanism and the structural change occurring when the defective γ-phase undergoes a thermal treatment under a pressure of 10^4 Pa oxygen are followed using thermogravimetry, electrical conductivity and infrared spectroscopy. The measuring device and the operating conditions have already been reported [2, 4, 5].

3. Results and discussion

3.1. Kinetic study

The kinetics of transformation were studied for $P_{O_2} = 10^4$ Pa by heating at a constant temperature between 500 and 600° C and observing the change in mass with time. Fig. 2 shows the kinetic curves during oxidation of two selected compositions, $x = 0.50$ and $x = 0.93$. These curves display a two-stage oxidation process. The initial pattern is a smooth parabolic curve, the amount oxidized (shown by an arrow in Fig. 2) being due to the experimental procedure. Briefly, the procedure was as follows: after oxidation of a sample at about 500° C, the gas was pumped out at the end of a run, the temperature was raised to the transformation temperature and oxygen was admitted at a pressure of 10^4 Pa. Thus, samples heated in this cycle and brought to the reaction temperature were partially reduced during the pumping period. As a result of this thermal treatment, a certain proportion of the manganese ions must be reduced to a lower valency, i.e. to Mn^{2+} ions. The parabolic curves correspond to the rapid reoxidation of these Mn^{2+} ions with the maintenance of spinel structure as confirmed by X-ray diffraction.

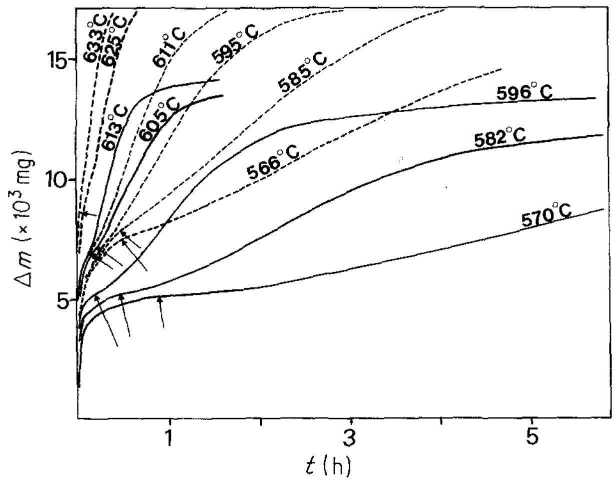

Figure 2 Kinetic curves in *TG* showing the two steps of oxidation at $P_{O_2} = 10^4$ Pa. The arrows indicate the change of kinetic law accompanying the transformation. ($-\, x = 0.50$, $---\, x = 0.93$).

For the second stage, corresponding to Mn^{2+} ions that are not totally oxidized in region I, the Δm against t plots are sigmoidal (Fig. 3) and the isotherms were best fitted with the equation $1\text{-}(1\text{-}\alpha)^{1/3} = kt$ between $0.2 < \alpha < 0.85$ (Fig. 4), where α, k and t are degree of precipitation, temperature-dependent proportionality constant and time, respectively. Such curves are usually explained on the basis of rapid nucleation but of no uniform probability with isotropic growth [6]. For a nucleation growth mechanism proceeding in spherical particles, the Mampel model from Delmon's charts [7] allows to introduce the B_s(i) parameter:

$$B_s(\mathrm{i}) = \pi v_0 r^2 \qquad (1)$$

where r is the mean grain radius, v_0 the number of nuclei and B_s(i) a characteristic magnitude for samples with spherical particles (index s) and an instantaneous nucleation (index i). B_s(i) is obtained by comparing the shape of the theoretical curves $\alpha = f(t/t_{1/2})$ for various B_s(i) values where $t_{1/2}$ is the half-reaction, with experimental curves. Following this comparison, B_s(i) being determined for each x value, the number of nuclei v_0 can be calculated from Equation 1. Also, in our case, v_0 was 5.2×10^{12} for $x = 0.50$ ($B_s(\mathrm{i}) = 200$) and 7.8×10^{12} for $x = 0.93$ ($B_s(\mathrm{i}) = 300$). For a given temperature it can be seen that v_0 increases with x, which is to be expected since the phase change is accompanied by an increase in the amount of oxidized phase due to the manganese ions. These ions may have a strong influence on the number of the nuclei.

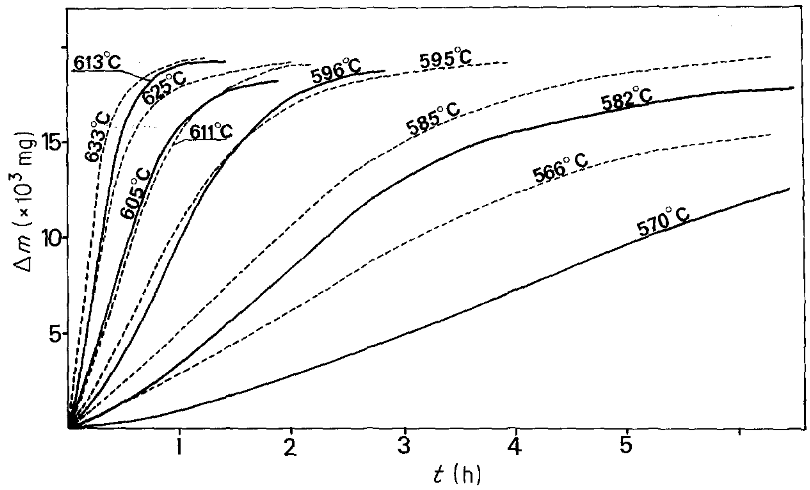

Figure 3 Effect of temperature on the reoxidation process. The plot shows the fractional transformation α against time curves. (—— $x = 0.50$, - - - $x = 0.93$).

An Arrhenius plot of the constant k against reciprocal temperature gives the activation energy of the transformation. The latter increases with x and exhibits one maximum for about $x = 0.50$ (Fig. 5). Then, higher Mn^{2+} concentration leads to a decrease of activation energy. The maximum observed is probably associated with the large non-stoichiometry for this composition comparatively to $x \approx 0$ and $x = 0.93$ substitution content as previously established [5]. However, the reported values for the transformation γ-$Fe_2O_3 \rightarrow \alpha$-$Fe_2O_3$ ($x = 0$) show a wide spread, from a minimum of 153 kJ mol^{-1} to a maximum of 360 kJ mol^{-1} [8, 9]. This failure to obtain consistent results has been attributed, among other factors, to the presence of impurities [9] and to the influence of particle size and shape [10].

The transformation from γ-defect phases to corundum structure can also be directly investigated by evaluating the behaviour of the electrical conductivity in region III. The kinetics of transformation were studied for $P_{O_2} = 10^4$ Pa by heating at constant temperature and observing the change in conductivity with time. Fig. 6 shows the kinetic curves during oxidation against composition x. As in thermogravimetry, the curves display a two-stage oxidation process due to the experimental procedure. The parabolic curves correspond to oxidation of Mn^{2+} ions generate during the thermal treatment and the phase may be considered as having a spinel structure. The linear portion represents the phase change but this method is not reliable as a measure of the weight change because in this region the electrical conductivity at the oxidation temperature is not related to the chemical composition in a single manner. It might be expected that the reaction rate will be firstly dependent of the amount of Mn^{2+} ions oxidized and secondly on the nature of the inversion products. This is particularly important with those samples which are not completely oxidized and there is a higher extent of manganese substitution in which the remaining Mn^{2+} ions form a manganese-rich spinel coexisting with a rhombohedral phase α-$(MnFe)_2O_3$, with orthorhombic phase Mn_2O_3.

3.2. Structural study by IR spectroscopy

The IR spectrum of the defective γ-phases is given in Fig. 7. The large number of absorption bands in the 270–800 cm^{-1} region may be attributed to the occurrence of a certain order in the vacancies and cation distribution on octahedral sites [5].

If these defective γ-phases are heated for more than 2 h at 700° C, the spectrum differs indicating a structural change (Fig. 8).

For composition $x < 0.72$, the spectrum exhibits the characteristic bands of α-Fe_2O_3 at 542, 470 and 324 cm^{-1} with only a slight slift with manganese content. This indicates that, instead of decomposing into the respective oxide α-Fe_2O_3 and Mn_2O_3, the

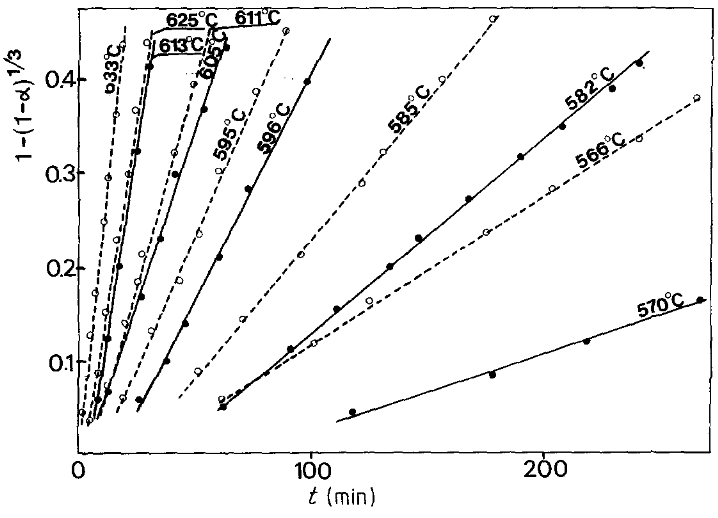

Figure 4 Plots of $1 - (1 - \alpha)^{1/3}$ against time. (—— $x = 0.50$, - - - $x = 0.93$).

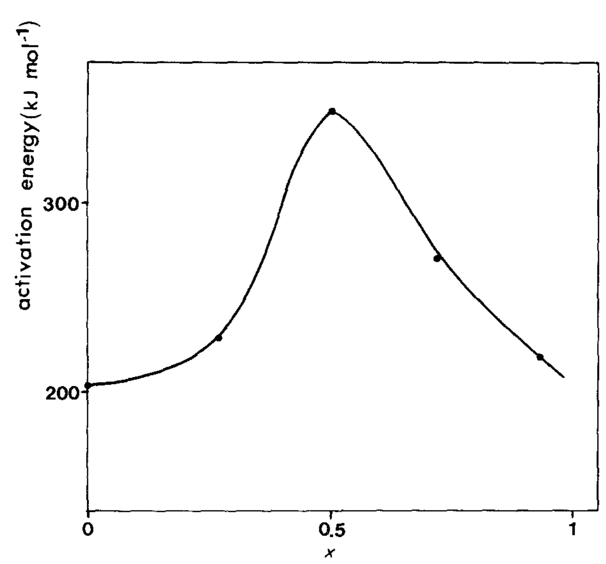

Figure 5 Variation of activation energy with composition.

defect phase γ is converted into the rhombohedral phase $\alpha\text{-(FeMn)}_2O_3$. The transformation defect phase $\gamma \rightarrow$ rhombohedral phase can be represented as follows

$$\gamma\text{-}[\mathrm{Mn}_{(8x)/(9-0.32x)}\mathrm{Fe}_{(24-8x)/(9-0.32x)}\square_{(3-0.96x)/(9-0.32x)}]\mathrm{O}_4$$
$$+\ \mathrm{O}_2 \rightarrow \alpha\text{-}[(12-4x)/(9-0.32x)\mathrm{Fe}_2\mathrm{O}_3,$$
$$(8x)/(9-0.32x)\mathrm{Mn}_2\mathrm{O}_3]$$

As the substitution extent was increased ($x = 0.72$), the spectra became quite complex as a result to the formation of a second phase (Fig. 8). The two other peaks around 670 and 560 cm^{-1} may be the formation of Mn_2O_3 with orthorhombic structure [11]. The formation of these two phases can be written as

$$[\mathrm{Mn}_{(8x)/(9-0.32x)}\mathrm{Fe}_{(24-8x)/(9-0.32x)}\square_{(3-0.96x)/(9-0.32x)}]\mathrm{O}_4$$
$$+\ \mathrm{O}_2 \rightarrow \alpha\text{-}[(12-4x)/(9-0.32x)\mathrm{Fe}_2\mathrm{O}_3,\ \mathrm{Y}\,\mathrm{Mn}_2\mathrm{O}_3]$$
$$+\ [(8x)/(9-0.32x)-\mathrm{Y}]\mathrm{Mn}_2\mathrm{O}_3$$

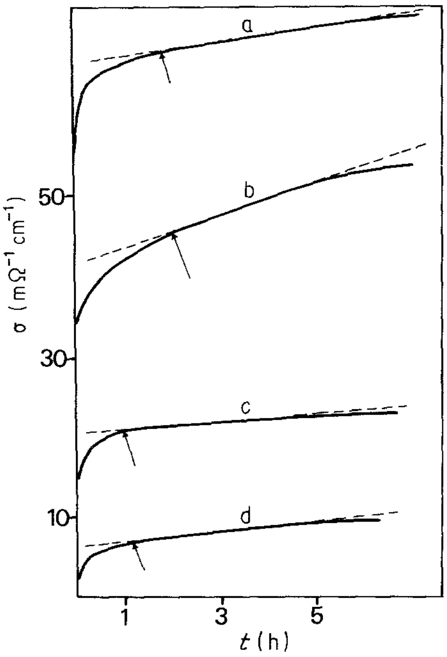

Figure 6 Kinetic curves in electrical conductivity showing the two steps of oxidation at $P_{O_2} = 10^4$ Pa. The arrows show the change of kinetic law due to the phase change. $T = 600°C$ (a $x = 0.93$, b $x = 0.50$, c $x = 0.27$, d $x = 0.14$).

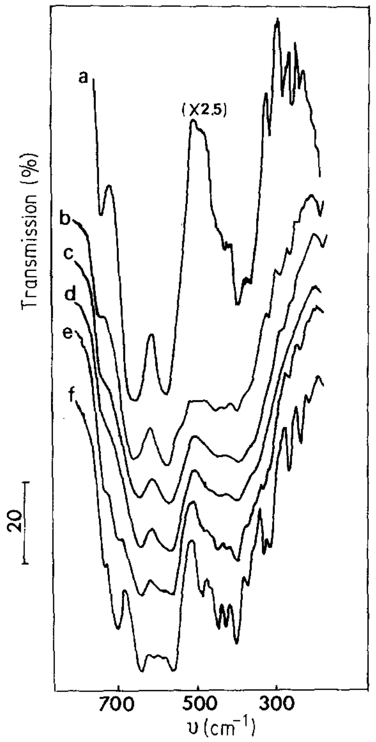

Figure 7 Infrared spectra of manganese cation deficient spinels at 450°C. (a $x = 0.97$, b $x = 0.97$, c $x = 0.72$, d $x = 0.67$ e $x = 0.37$, f $x = 0.14$).

In addition, over the range examined, the intensity ratio I_x/I_0 of the 324 cm^{-1} band, where I_0 is the intensity of pure $\alpha\text{-Fe}_2O_3$ band and I_x the intensity of solid solution $\alpha\text{-(Fe, Mn)}_2O_3$ band, linearly decreases as the extent of substitution x increases (Fig. 9). It is then possible to determine the unknown substitution extent of a α-phase.

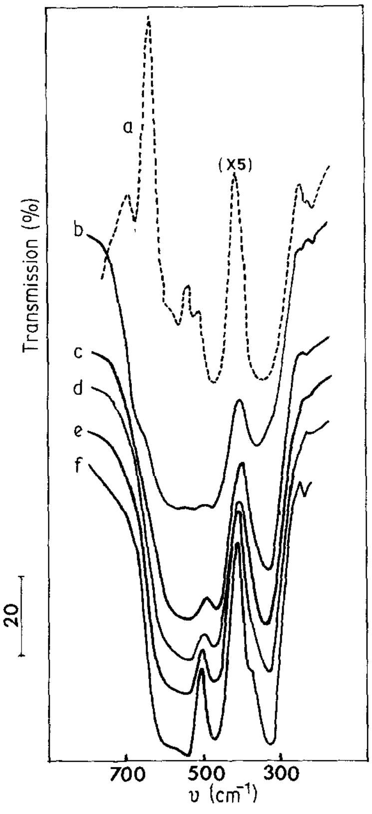

Figure 8 Infrared spectra of transformation products after heating at 700°C. (a $x = 0.97$, b $x = 0.97$, c $x = 0.72$, d $x = 0.67$, e $x = 0.37$, f $x = 0.14$)

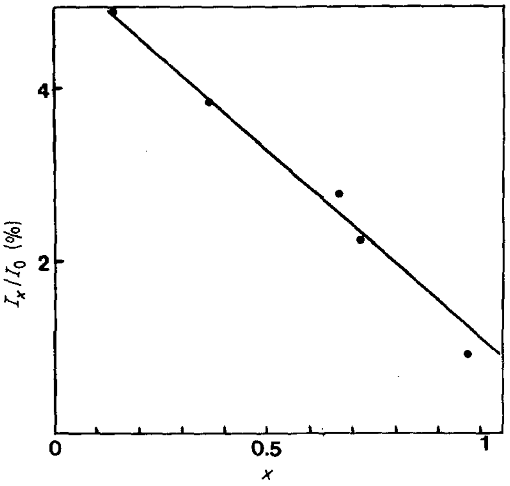

Figure 9 Evolution of the intensity ratio I_x/I_0 of the 324 cm^{-1} band as a function of manganese-substitution extent x.

Figs 10 and 11 shows the evolution of the IR spectrum plotted against temperature of the γ-phases for two composition $x = 0.37$ and $x = 0.93$. At temperatures below 700° C but above the oxidation temperature into γ-phase (400° C), the conversion $\gamma \rightarrow \alpha$ occurs progressively with temperature. By fixing the oxidation time, it is possible to evaluate a transition temperature for each composition by noting the temperature T_{tr} at which the 470 cm^{-1} peak of the α-phase appears. The variation of T_{tr} with composition is shown in Fig. 12 and expresses an increase in the stability of the γ-phases with Mn-substitution extent. However, because of the oxidation of Mn^{2+} to Mn^{3+} ions and to the affinity of Mn^{3+} ions for octahedral sites, the stabilization of these defect phases containing cobalt or zinc (Fig. 12). In the corundum structure, Mn^{3+} ions with the outer electronic configuration $t_{2g}^3 e_g^1$ are located in a favourable octahedral environment [12].

4. Conclusion

This study reveals that during oxidation of defective manganese substituted magnetites above 500° C, a phase change from the spinel to the corundum structure occur. The kinetic curves related to the phase change show that the transformation can be described by the equation $1 - (1 - \alpha)^{1/3} = kt$ indicating a nucleation growth mechanism with a process characterized by an activation energy depending of the composition. The lower activation energy for high manganese concentration can be attributed to the larger amount of Mn^{3+} ions created by reoxidation which involve instability of the spinel structure.

Infrared investigation of the transformation enables us to conclude that the decomposition of defect phases γ takes place in two steps. In the first step, the IR spectrum of oxidation products obtained for $x < 0.72$ exhibits the absorption bands of the α-Fe_2O_3 phase with only a slight shift suggesting the formation of a rhombohedral phase α-$(FeMn)_2O_3$. In the second step for $x > 0.72$, orthorhombic Mn_2O_3 is formed in addition to $\alpha(FeMn)_2O_3$.

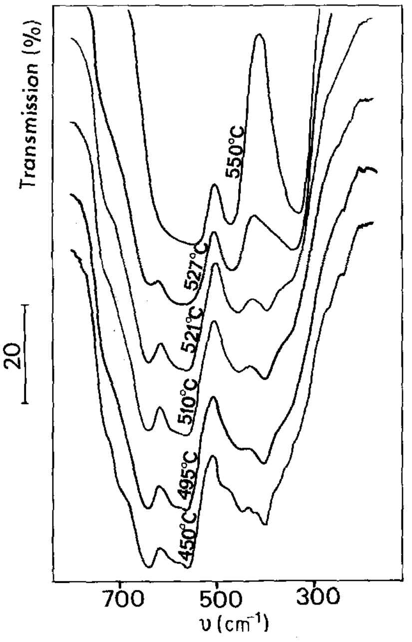

Figure 10 Evolution plotted against temperature of the IR spectrum of the γ phase of composition $x = 0.37$.

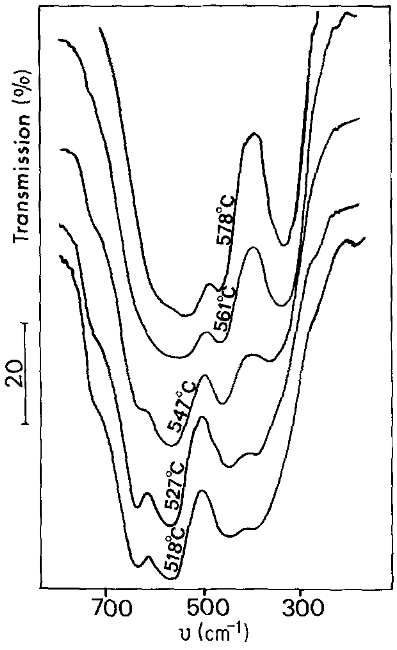

Figure 11 Evolution plotted against temperature of the IR spectrum of the γ phase of composition $x = 0.93$.

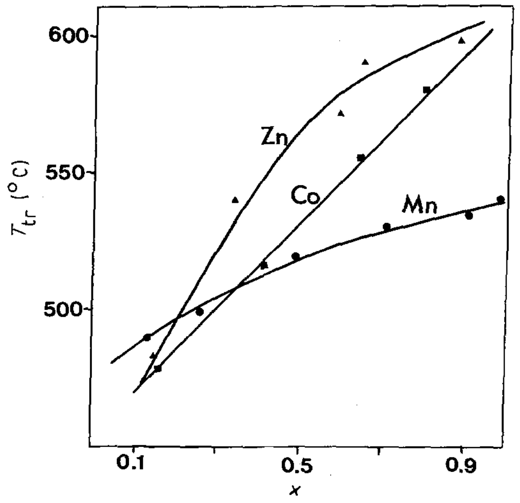

Figure 12 Variation of transformation temperature with composition for different defective spinels.

References

1. P. TAILHADES, M. EL GUENDOUZI, A. ROUSSET and B. GILLOT, *C. R. Acad. Sci., Paris, Série II* **299** (1984) 13.
2. B. GILLOT, M. EL GUENDOUZI, P. TAILHADES and A. ROUSSET, *React. Solids* **1** (1986) 139.
3. E. H. L. J. DEKKER and G. D. RIEK, *Rev. Int. Hautes Temp. Refract.*, **11** (1974) 187.
4. B. GILLOT, M. EL GUENDOUZI, A. ROUSSET and P. TAILHADES, *J. Mater Sci.* **21** (1986) 2926.
5. M. EL GUENDOUZI and B. GILLOT, *Mater. Chem. Phys.* **13** (1985) 179.
6. K. L. MAMPEL, *Z. Phys. Chem. A* **187** (1940) 43.
7. B. DELMON, "Introduction à la Cinétique Hétérogène", (Technip, Paris, 1969).
8. S. KACHI, K. MOMIYAMA and S. SHIMIZU, *J. Phys. Soc. Jpn* **18** (1963) 106.
9. F. E. DE BOER and P. W. SELWOOD, *J. Amer. Chem. Soc.*, **76** (1954) 3365.
10. W. FEITKNECHT and U. MANNWEILER, *Helv. Chim. Acta* **50** (1967) 570.
11. W. B. WHITE and V. G. KERAMIDAS, *Spectrochim. Acta* **28A** (1971) p. 501.
12. A. NAVROTSKY and O. KLEPPA, *J. Inorg. Nucl. Chem.* **29** (1967) 2701.

Received 5 October 1987
and accepted 26 January 1988